Transversal Distribution of Acyl-Linked Pyrene Moieties in Liquid-Crystalline Phosphatidylcholine Bilayers. A Fluorescence Quenching Study†

Massimo Sassaroli,*,‡ Mika Ruonala,§ Jorma Virtanen,|| Matti Vauhkonen,§ and Pentti Somerharju*,§

Department of Physiology and Biophysics, Mount Sinai School of Medicine, New York, New York 10029-6574, Institute of Biomedicine, Department of Medical Chemistry, University of Helsinki, Siltavuorenpenger 10A, P.O. Box 8, 00014 Helsinki, Finland, and Department of Chemistry, University of California, Irvine, California 92717

Received February 2, 1995; Revised Manuscript Received April 13, 1995⊗

ABSTRACT: Quenching of the fluorescence of pyrene-labeled phospholipids by dibromolipids was used to determine the chain length dependence of the bilayer depths of the pyrenyl moieties. Six 1-palmitoyl-2-(pyrenyl-*n*-acyl)-phosphatidylcholines (Pyr_nPC) were examined, with end-labeled pyrenyl chains varying in length, *n*, from 4 to 14 carbons. These lipids were incorporated, at a concentration of 0.3 mol %, into bilayers composed of various mixtures of 1-palmitoyl-2-oleoylphosphatidylcholine (POPC) and of one of three 1-palmitoyl-2-(*x,y*-dibromostearoyl)phosphatidylcholine quencher lipids ($Br_{x,y}PC$; x,y = 6,7; 9,10; or 11,12). Parallel experiments were carried out with bilayers containing 50 mol % cholesterol. Quenching in these systems is dynamic, as demonstrated by the identical dependence of steady-state fluorescence intensities and excited state lifetimes of Pyr_8PC on the mole fraction of $Br_{6,7}PC$. Stern−Volmer analysis of the $Br_{x,y}PC$ mole fraction dependence of Pyr_nPC fluorescence yielded apparent quenching constants, K_{SV}, which show a systematic relation with both the length of the pyrenyl acyl chain and the position of the bromine atoms. The quenching data were further analyzed by plotting K_{SV} as a function of *n* (defined above), or *b* (the average of the two bromine positions for each Pyr_nPC), or $n - b$ (the separation between pyrenes and bromines). In all cases, the data were fit by Gaussian functions yielding estimates of the centers and the apparent 1/*e* half-widths of the transversal distributions of the pyrenyl moieties in methylene units (mu). Both in the absence and in the presence of cholesterol, the position of each Pyr_nPC Gaussian center is equal to the sum of *n* plus a constant $d \approx 2.5$ mu, corresponding to the distance from the effective center of the pyrenyl moiety to its point of attachment to the acyl chain. However, consistent with the well-documented cholesterol-induced conformational ordering of the acyl chains, addition of 50 mol % cholesterol to the bilayers results in a considerable reduction of the 1/*e* half-widths of the distributions, from ≈9 mu in its absence to ≈5 mu. The good agreement between measured and predicted equilibrium depths of the pyrenyl moieties indicates that these Pyr_nPC lipid analogues mimic their natural precursors more closely than others labeled with more polar fluorophores, which show a marked tendency to partition to the membrane surface.

Fluorescent lipid analogues have been used extensively to investigate many aspects of membrane biophysics and related phenomena. Among them, pyrene-labeled phospholipids have been widely utilized to measure, for instance, lipid lateral diffusion (Galla et al., 1979; Eisinger et al., 1986; Sassaroli et al., 1990) and distribution (Galla & Sackmann, 1975; Hresko et al., 1986; Somerharju et al., 1985; Tang & Chong, 1992), spontaneous or protein mediated lipid transport (Roseman & Thompson, 1980; Pownall & Smith, 1989; Somerharju et al., 1987), phospholipid hydrolysis (Hendrikson & Rauk, 1981; Thuren et al., 1984) and conformation (Eklund et al., 1992). They have also been used to detect the presence of lipid domains in cell membranes (Dix & Verkman, 1990) and to determine the position of membrane protein tryptophan residues by resonance energy transfer (RET)[1] (Bastiaens et al., 1990).

However, despite the large number of applications, surprisingly few studies have attempted to characterize the properties of the pyrenyl lipids themselves: for instance, the precise depths at which the pyrenyl moieties of these derivatives reside within the bilayer are still unknown. Such information is essential to establish whether or not the pyrene probe perturbs the conformation of the acyl chain to which it is attached, as found in the case of nitrobenzoxadiazole (NBD), another commonly used fluorophore (Chattopadhyay & London, 1987; Wolf et al., 1992). Furthermore, when pyrenyl lipids are used in RET experiments, the accuracy with which the membrane protein tryptophans or other

†This work was supported by grants from the Sigrid Juselius Foundation, the Finnish Academy (to P.S.), and the Finnish Cultural Foundation (to J.V.). A preliminary report of this work was presented at the 38th Annual Meeting of the Biophysical Society, New Orleans, LA (Virtanen et al., 1994).

* Address correspondence to these authors. For M.S.: E-mail, sassaroli@msvax.mssm.edu; Telephone, 212-241-9512; Fax, 212-860-3369. For P.S.: E-mail, somerharju@katk.helsinki.fi; Telephone, 358-0-1918216; Fax, 358-0-1918276.

‡ Mount Sinai School of Medicine.

§ University of Helsinki.

|| University of California.

⊗ Abstract published in *Advance ACS Abstracts,* June 15, 1995.

[1] Abbreviations: $Br_{x,y}PC$, 1-palmitoyl-2-(x,y-dibromostearoyl)phosphatidylcholine, where x,y are the positions of the two bromine atoms in the *sn*-2 acyl chain; *mu*, methylene units; Pyr_nPC, 1-palmitoyl-2-(pyrenyl-*n*-acyl)phosphatidylcholine, where *n* is the length of the pyrene-labeled acyl chain in *mu*; POPC, 1-palmitoyl-2-oleoylphosphatidylcholine; NBD, *N*-7-nitro-2,1,3-benzoxadiazole; TEN, Tris−EDTA−NaCl buffer; K_{SV}, apparent Stern−Volmer quenching constant; HPLC, high-performance liquid chromatography; TLC, thin-layer chromatography; RET, resonance energy transfer.

0006-2960/95/0434-8843$09.00/0

fluorophores of interest can be located depends critically on the accuracy with which the depth of the pyrenyl moiety within the bilayer is known (Eisinger et al., 1984; Bastiaens et al., 1990).

Two methods have been mainly applied to estimate fluorophore depths within membranes. One of them makes use of RET between suitable pairs of donor and acceptor moieties (Kleinfeld, 1985; Wolf et al., 1992). However, determination of depth by this method is often problematic because the data analysis is quite complex and, more important, because the exact transversal location of the acceptor or donor used as a depth reference is generally not well established. The second, more common approach makes use of quenching of the fluorophore of interest by spin-labeled probes or bromine atoms attached to specific positions along the acyl chains of phospholipids or fatty acids (Tennyson & Holloway, 1986; Bolen & Holloway, 1990; Abrams & London, 1992; Abrams et al., 1992). Brominated phospholipids offer a major advantage over other quenchers because the transversal distribution of the bromine atoms has been established by X-ray diffraction methods (McIntosh & Holloway, 1987; Wiener & White, 1991). In addition, their physical properties are similar to those of the unsaturated precursors (East & Lee, 1982). Therefore, it is possible to determine the fluorophore distribution with high accuracy by proper analysis of the quenching data.

In most published reports, quantitative analysis of the quenching data is carried out by use of the parallax method, developed by London and coworkers (Chattopadhyay & London, 1987; Abrams & London, 1992, 1993). While this method is capable of providing accurate estimates of fluorophore depths, it is based on two main assumptions that may limit its generality: (i) quenching is considered to occur via a static mechanism and (ii) both quenchers and fluorophores are assumed to be located at unique depths within the bilayer. As will be shown below, quenching of the fluorescence of pyrenyl residues by bromines is dynamic. Furthermore, both experimental (McIntosh & Holloway, 1989; Wiener & White, 1992) and theoretical results (De Loof et al., 1991; Pearce & Harvey, 1993) indicate that acyl chain methylenes are not confined to fixed locations, but are free to span a broad range of depths within the bilayer. For these reasons, the parallax method is not suitable to the analysis of our quenching data.

We have previously modeled the intramolecular excimer formation of dipyrenylphosphatidylcholines in bilayers by using a Gaussian function to describe the depth distributions of the pyrenyl residues (Eklund et al., 1992). Since both intramolecular excimer formation and quenching of pyrene by bromolipids result from dynamic, collisional processes, it is appropriate to extend this previously developed formalism to the analysis of the quenching data. Accordingly, we derive a simple Gaussian equation and use it to analyze the quenching of pyrene bound to the terminal methyl of the *n*-carbon-long *sn*-2 acyl chain of phosphatidylcholine (Pyr_nPC, $n = 4-14$ carbons) by PCs having one bromine atom attached to each of two adjacent carbons of their *sn*-2 stearoyl chain ($Br_{6,7}$PC, $Br_{9,10}$PC, or $Br_{11,12}$PC, respectively). The equilibrium depths of the various pyrenes are found to be a smooth and predictable function of the length of the labeled chains, indicating that the pyrene distribution within the bilayer is dictated by the length of the acyl chain and not by steric constraints or other intrinsic properties of the probe. Addition of 50 mol % cholesterol (cholesterol/PC mole ratio = 1.0) to the bilayer does not significantly affect the average depths, but causes a considerable reduction in the widths of the distributions.

EXPERIMENTAL PROCEDURES

Lipids and Other Reagents. 1-Palmitoyl-2-oleoylphosphatidylcholine (POPC) was purchased from Avanti Polar Lipids (Birmingham, AL) and cholesterol (99+ grade) from Sigma (Deisenhofen, Germany), and both were found to be pure by TLC analysis. The 1-palmitoyl-2-(pyrenyl-*n*-acyl)-phosphatidylcholine derivatives (Pyr_nPCs) were synthesized and purified as described previously (Somerharju et al., 1987). 1-Palmitoyl-2-(*x,y*-dibromostearoyl)phosphatidylcholines ($Br_{x,y}$PCs) were synthesized by bromination of 1-palmitoyl-2-petrosellenyl-, -oleoyl-, or -vaccenylphosphatidylcholines (Dawidowicz & Rothman, 1976) and purified by two consecutive HPLC runs on a preparative silica column using chloroform/methanol/water (60:30:4 by volume) as the solvent. $Br_{x,y}$PCs were homogeneous on TLC, and gas chromatographic analysis of the acyl residues as methyl esters showed that the 18:1 fatty acid/palmitate ratio of each purified bromolipid was less than 0.04, indicating that bromination was nearly complete (>96%) in all cases. We note that the data analysis methods used below to determine the depth distribution of the pyrene moieties are insensitive to minor variations in the degree of lipid bromination (see Results). The positional purities of Pyr_nPCs or $Br_{x,y}$PCs were not determined, but the method used to synthesize the asymmetric PC precursors typically provides >95% of the nominal compound (Mason et al., 1981; Somerharju et al., 1987). The concentrations of $Br_{x,y}$PCs and POPC were determined by a phosphate assay (Rouser et al., 1970) and the concentrations of Pyr_nPCs by absorbance measurement using 42 000 cm^{-1} M^{-1} as the extinction coefficient of pyrene at 342 nm in ethanol (Somerharju et al., 1985). The concentration of cholesterol was determined gravimetrically.

Preparation of Lipid Vesicles. Stock mixtures of $Br_{x,y}$-PC/POPC in various ratios with or without 50 mol % cholesterol (cholesterol/PC mole ratio = 1.0) were prepared in chloroform and stored in the dark at −30 °C. To prepare the vesicles, 50 nmol of the stock mixtures was dispensed, using a microsyringe, into solvent-washed glass tubes containing 200 μL of chloroform followed by the addition of 0.3 mol % of Pyr_nPC. The solvent was then evaporated under a nitrogen stream, and the samples were kept under high vacuum for 1 h to remove any residual solvent. Then 1 mL of TEN (20 mM Tris-HCl, 1 mM EDTA, 150 mM NaCl, pH 7.4) buffer was added under argon, and the tubes were vortexed for 5 s. After equilibration in the dark at room temperature for 30 min, the samples were sonicated for 10 s at 55 W output with a Branson B-12 sonifier (Branson Inc., Danbury, CT) equipped with a microtip and then equilibrated at 25 °C for 1 h before the fluorescence measurements.

Steady-State and Time-Resolved Fluorescence Measurements. Steady-state fluorescence intensities were measured by use of a Hitachi F-4000 fluorescence spectrophotometer or a laboratory-modified, computer-controlled SLM spectrofluorometer (SLM Instruments Inc., Urbana, IL) equipped with a thermostatically controlled cuvette holder. The

fluorescence of the pyrene monomer was measured using excitation and emission wavelengths of 344 and 378 nm, respectively, and 5 nm bandwidths. The pyrene monomer excited state lifetimes were measured by the time-correlated single photon counting method using an IBH Model 5000 time-resolved fluorometer (IBH Consultants Ltd., Glasgow, Scotland, U.K.) equipped with a coaxial flashlamp and a thermostated sample holder. Excitation light at 316 or 337 nm from the nitrogen-filled flashlamp and fluorescence emission at 395 nm were selected by monochromators. In addition, two long-pass filters (UV-36 and UV-37, Hoya Optics Inc., Fremont, CA) were used in the emission path to reduce scattering and stray light artifacts. The decay data were not corrected for background fluorescence. Analysis of the time-resolved decays was carried out using the nonlinear least-squares iterative reconvolution method. All steady-state and time-resolved measurements were performed with vesicle suspensions equilibrated in air at 25 °C.

DATA ANALYSIS

The first step in our data analysis consisted of applying the Stern−Volmer equation (Lakowicz, 1983) to derive the apparent Stern−Volmer quenching constant, K_{SV}, from the $Br_{x,y}PC$ mole fraction dependence of the steady-state fluorescence intensities of each Pyr_nPC. In eq 1, F_0 and F

$$F_0/F = 1 + K_{SV}X = 1 + k_Q\tau_0X \quad (1)$$

represent the emission intensities in the absence and presence of $Br_{x,y}PC$ quencher, respectively, k_Q is the bimolecular quenching constant, which is proportional to the fluorophore−quencher collision frequency, τ_0 is the Pyr_nPC excited state lifetime in the absence of quencher, and X is the quencher concentration expressed as mole fraction of the total lipid.

The values of F_0 were, within experimental error, equal for all Pyr_nPC species used in this study, suggesting that the values of τ_0 are also equal. Therefore, we could calculate k_Q for all $Pyr_nPC/Br_{x,y}PC$ combinations, even though we have measured τ_0 only for Pyr_8PC. However, proper determination of k_Q would also require the estimation, approximate at best, of the molar concentrations of both pyrene moieties and bromine atoms within the membrane, rather than the mole fractions used in eq 1. Since, for the purpose of this study, we are only interested in the dependence of quenching on the relative depths of pyrene and bromine and not in the detailed determination of collision frequencies and diffusion coefficients, the additional complications and uncertainties in the calculation of k_Q are not justified. For this reason, throughout this report we have chosen to use the apparent K_{SV} rather than k_Q.

We have previously used a Gaussian equation to model the dependence of the efficiency of intramolecular excimer formation in dipyrenylphosphatidylcholines as a function of the difference in length of the two acyl chains bearing the pyrene moieties (Eklund et al., 1992). Since both the intramolecular excimer formation and the quenching of pyrene fluorescence by dibromolipids studied here result from depth-dependent, collisional events and, therefore, can be considered formally analogous, we use the previously derived Gaussian equation with minor modifications to analyze the new quenching data. The following is the basic equation used in our analysis:

$$K_{SV} = K_{max}e^{-[(a-b)/h]^2} \quad (2)$$

where a and b represent the equilibrium distances from the bilayer−water interface to the effective center of the pyrenyl moiety and the midpoint between the two bromine atoms, respectively, measured in terms of methylene units (mu); h is the $1/e$ half-width of the Gaussian distribution, and K_{max} is the maximum value of K_{SV} which is obtained when $a = b$. The distance a can be considered as the sum of two components:

$$a = n + d \quad (3)$$

where n represents the number of methylene units in the pyrenyl acyl chain and d is the additional distance, also measured in mu, from the effective center of the pyrenyl moiety to its site of attachment to the acyl chain. Thus, eq 2 transforms to

$$K_{SV} = K_{max}e^{-[(n+d-b)/h]^2} \quad (4)$$

It is important to note that the parameter h represents only an *apparent* value of the distribution $1/e$ half-width, which includes contributions from the physical sizes of both pyrenyl probes and bromine atoms as well as from the dynamic broadening due to their motions. A schematic representation of the molecular framework, including the distances defined above, is shown in Figure 1.

A somewhat similar approach, also based on a Gaussian distribution analysis, has been described by others and applied to determine the bilayer depths of tryptophan residues of membrane-bound proteins (Ladokhin, 1993; Tretyachenko-Ladokhina et al., 1993).

RESULTS

Mechanism of Quenching of Pyr_nPC Fluorescence by $Br_{x,y}PCs$. As discussed above, one of the premises of the parallax method is that quenching occurs via a static mechanism. While this is a reasonable approximation when fluorophores with short lifetimes are used, the same may not be true for probes with long-lived excited states, such as pyrene. Therefore, in order to determine the quenching mechanism operative in our system, we measured both the excited state lifetimes, τ, and the steady-state intensities, F, of Pyr_8PC incorporated into POPC bilayers containing various mole fractions of $Br_{6,7}PC$. These values, normalized to those measured in the absence of quencher, τ_0 and F_0, are plotted in Figure 2.

In the absence and in the presence of $Br_{6,7}PC$ at all mole fractions examined, Pyr_8PC exhibited multiexponential intensity decays, the best fits to the data being obtained using three components. The shortest lifetime (1.6−2.0 ns) was unaffected by quenchers, and its relative amplitude was strongly excitation wavelength dependent, being approximately twice as large with excitation at 316 nm than at 337 nm. A lifetime component with the same value was also recovered from the analysis of the fluorescence decays of unlabeled POPC vesicle suspensions both in distilled water and in TEN buffer, which indicates that this fluorescence probably originates from contaminants in the lipid or in the organic solvents used to prepare the vesicles. This component was therefore deemed to arise from background fluorescence and disregarded.

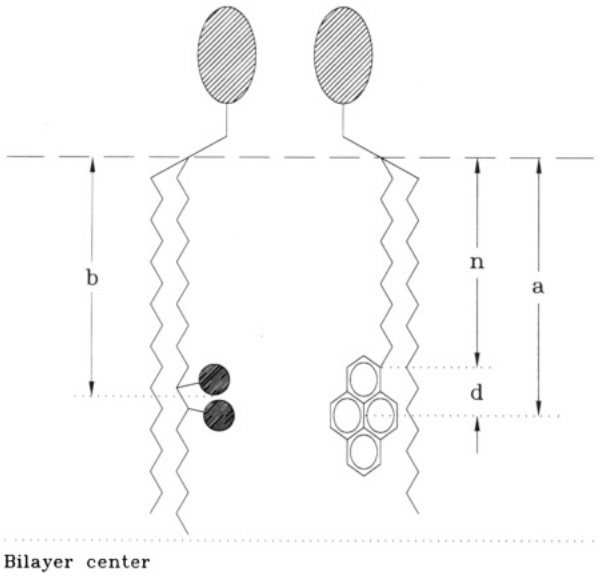

FIGURE 1: Schematic representation of the structures of Pyr_nPC and $Br_{x,y}PC$ species and definition of the parameters used in the analysis of the quenching data. For Pyr_nPC (on the right), n represents the distance from the bilayer−water interphase to carbon-1 of the pyrenyl moiety, d is the distance from this carbon to the center of the pyrenyl moiety, and $a = n + d$ is the distance from the bilayer−water interphase to the effective center of the pyrene. For $Br_{x,y}PC$ (on the left) b represents the distance from the bilayer-water interphase to the midpoint between the two bromine atoms. All these distances are measured in methylene units (mu).

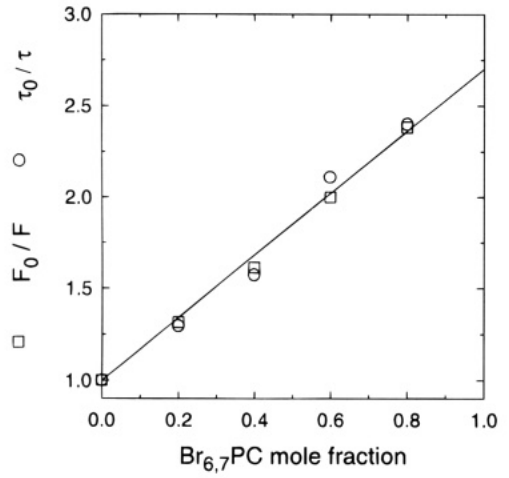

FIGURE 2: Dependence of the relative values of fluorescence steady-state intensities (F_0/F) and lifetimes (τ_0/τ) of Pyr_8PC on the mole fraction of $Br_{6,7}PC$ in POPC bilayers. F_0 and τ_0 are the values of steady-state intensity and lifetime, respectively, measured in neat POPC bilayers. The line represents the best fit to the data using eq 1.

The intermediate component in the Pyr_8PC fluorescence decays (15−25 ns) was also insensitive to the presence of quencher lipids and accounted for ≈ 2% of the fluorescence intensity in neat POPC vesicles and up to ≈10% in the vesicles containing 0.8 mol fraction $Br_{6,7}PC$. A decay component with a similar lifetime was also recovered from the unlabeled POPC vesicle suspensions. Although its fractional contribution to the Pyr_8PC decays as a function of $Br_{6,7}PC$ concentration is difficult to assess, we believe that the intermediate lifetime component also arises from background fluorescence.

Only the third and longest lifetime, which accounted for most of the fluorescence emission with either excitation wavelength, displayed a consistent dependence on the concentration of quencher. Therefore, the relative values of the fluorescence lifetime of Pyr_8PC, τ_0/τ, as a function of $Br_{6,7}PC$ mole fraction, plotted in Figure 2, were calculated solely on the basis of this longest lifetime component, which has a value of 122.4 (±8.2) ns in pure POPC bilayers, in good agreement with that previously measured for $Pyr_{10}PC$ in POPC bilayers (Vauhkonen et al., 1990). To test whether including the contribution of the intermediate lifetime component would lead to significant deviations from the values shown, intensity-weighted average lifetimes, $\langle t \rangle = \sum\alpha_i\tau_i^2/\sum\alpha_i\tau_i$, were calculated using the intermediate and long lifetime components and their fractional amplitudes, α. In all cases, the resulting values of $\langle\tau\rangle$ were ≤4 ns lower than the respective long τ, while $\langle\tau_0\rangle/\langle\tau\rangle$ differed by <2% from τ_0/τ.

As shown in Figure 2, the relative values of steady-state intensity and time-resolved lifetime at all $Br_{6,7}PC$ mole fractions are in excellent agreement, demonstrating that quenching in this system occurs via a dynamic, collisional process (Lakowicz, 1983). Further support for this conclusion is provided by the observation (data not shown) that saturating the liposome suspensions with oxygen, which markedly shortens the pyrene lifetime (Fischkoff & Vanderkooi, 1975; Chong & Thompson, 1985), results in a major reduction of the quenching efficiency (≈80% decrease in K_{SV}) of the bromolipids, as expected for a dynamic process.

Determination of the Transversal Distribution of Pyrenyl Moieties as a Function of Pyr_nPC Acyl Chain Length. The $Br_{x,y}PC$ mole fraction dependence of the steady-state fluorescence intensity of Pyr_nPC was determined for all combinations of quencher and fluorophore-labeled PCs, as well as both in the absence and in the presence of 50 mol % cholesterol within the bilayers. All measurements were repeated on two independent sets of samples. Representative data are shown in Figure 3, together with the best-fit lines calculated using eq 1; the slopes of the lines give the values of K_{SV}, the apparent Stern−Volmer quenching constants.

Subsequent analysis of the data to determine the mean transversal position and width of the distribution of each pyrenyl moiety was carried out using three approaches. In the first, the K_{SV} values were plotted as a function of n, the number of methylene units of the pyrene-linked acyl chain for each $Br_{x,y}PC$ matrix, as shown in Figure 4. A few qualitative observations can be made by simple inspection of this figure: First, the efficiency of quenching by each $Br_{x,y}PC$ varies with the length of the pyrenyl acyl chain. Second, the length of the pyrenyl chain yielding maximal quenching correlates with the location of the bromine atoms. Third, K_{max}, the maximum value of K_{SV}, decreases with increasing depth of the bromine atoms. Quantitative analysis of these data was carried out by nonlinear least-squares fitting of the data to eq 4. The lines in Figure 4 represent the best fits to the data calculated using this equation and the optimized parameters K_{max}, d, and h listed in Table 1. As noted in the legend to Table 1, the analysis of the $Br_{6,7}PC$ data was carried out by setting the parameter h equal to the average of the values obtained for the $Br_{9,10}PC$ and $Br_{11,12}PC$ data sets and holding it fixed during the iterative fitting procedure. Failure to do so, particularly for the data in the absence of cholesterol, resulted in numerical values of d and h which were inconsistent with those obtained from the other two brominated PCs or by using the other methods of data

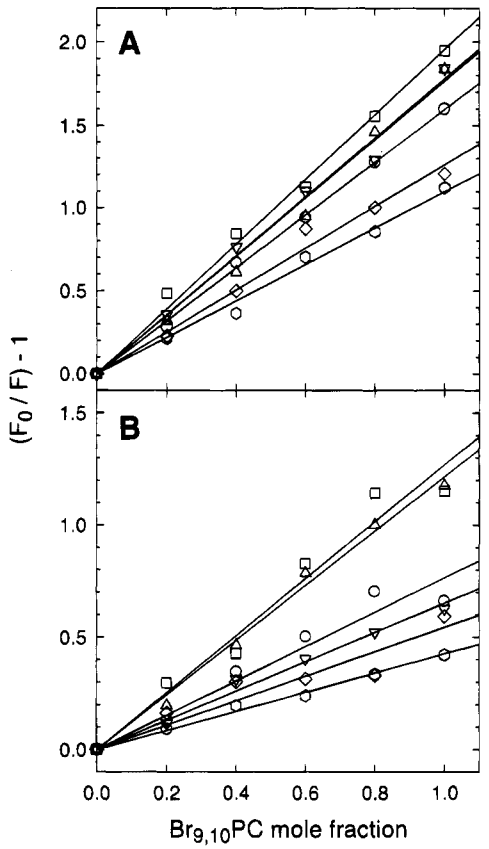

FIGURE 3: Dependence of the relative fluorescence intensity of Pyr_n-PCs on the mole fraction of $Br_{9,10}PC$ in POPC bilayers without (A) or with (B) 50 mol % cholesterol. The symbols refer to Pyr_4-PC (circles), Pyr_6PC (squares), Pyr_8PC (triangles), $Pyr_{10}PC$ (inverted triangles), $Pyr_{12}PC$ (diamonds), and $Pyr_{14}PC$ (hexagons). The lines represent the best fits to the data using eq 1.

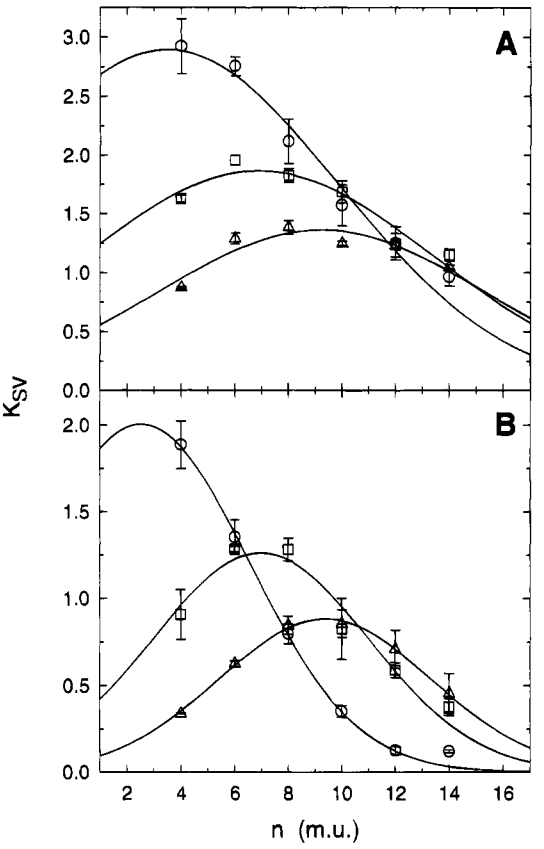

FIGURE 4: Dependence of K_{SV}, the apparent Stern–Volmer quenching constant, on n, the number of methylene units in the pyrenylacyl chains, for bilayers with different $Br_{x,y}PC$ quenchers. The quencher lipid was $Br_{6,7}PC$ (circles), $Br_{9,10}PC$ (squares), or $Br_{11,12}PC$ (triangles). Bilayers contained no (A) or 50 mol % cholesterol (B). The solid lines are the best fits to eq 4 using the parameters listed in Table 1. Note that K_{max}, the maximal value of K_{SV}, depends on the position of the bromine atoms in the *sn*-2 acyl chain of the quencher lipid.

analysis described below. In our opinion, the most likely cause for this inconsistency is the lack of a well-defined maximum in the $Br_{6,7}PC$ data set, which leads to an exaggerated sensitivity of the best-fit parameters to the experimental uncertainties. The quality of the fit using the fixed h is not substantially worse than that obtained with all parameters floating, with slightly larger discrepancies between calculated and experimental K_{SV} values only for n = 12 and 14.

In the absence of cholesterol, the average value of d, the distance from the effective center of the pyrenyl moiety to its site of attachment to the acyl chain, is 2.6 mu (Table 1), which, assuming an average length per methylene unit of 0.9 Å (McIntosh & Holloway, 1987), is equivalent to a distance of ≈2.4 Å. This value is in good agreement with that of ≈2.8 Å deduced from the X-ray structure of pyrene (Robertson & White, 1947), strongly suggesting that the mean transversal positions of the pyrenes are determined mainly by the lengths of the chains to which they are attached. Interestingly, addition of 50 mol % cholesterol affects only slightly the depths of the pyrenes relative to the bromines, since the mean value of d is found to be 2.9 mu, equivalent to 3.1 Å, assuming an average length per methylene unit of 1.08 Å on the basis of a 20% increase in bilayer thickness in the presence of cholesterol (Lecuyer & Dervichian, 1969).

In the absence of cholesterol, the distributions are quite broad, as indicated by the mean value of h = 9.0 mu (Table

Table 1: Pyrene Distribution Parameters Obtained from the Dependence of K_{SV} on n, the Pyrenylacyl Chain Length in mu

	POPC[a]				+50 mol % cholesterol[b]			
	d[c] (mu)	h[d] (mu)	h_{pyr}[e] (mu)	K_{max}[f]	d (mu)	h (mu)	h_{pyr} (mu)	K_{max}
$Br_{6,7}PC$	3.0	9.0[g]	6.4	2.90	4.0	5.7[g]	4.0	2.00
$Br_{9,10}PC$	2.6	9.3	6.6	1.87	2.5	5.7	4.0	1.26
$Br_{11,12}PC$	2.3	8.7	6.2	1.36	2.1	5.6	4.0	0.88
mean	2.6 ± 0.4	9.0 ± 0.3	6.4 ± 0.2		2.9 ± 1.0	5.7 ± 0.05	4.0 ± 0.04	

[a] The bilayers consisted of POPC and $Br_{x,y}PC$ in variable molar ratios. [b] The bilayers consisted of POPC and $Br_{x,y}PC$ in variable molar ratios and 50 mol % cholesterol (cholesterol/phospholipid mole ratio = 1.0). [c] The effective distance of the pyrene center to the site of attachment to the acyl chain (see Figure 1). [d] The 1/*e* half-width of the pyrene Gaussian: as discussed in the text, this value includes contributions from the physical sizes of pyrene and bromines, as well as broadening effects due to their motions. [e] The 1/*e* half-width of the pyrene Gaussian reduced by a factor of $1/\sqrt{2}$ (see Discussion). [f] The maximum value of K_{SV} in each $Br_{x,y}PC$ matrix obtained by fitting the data according to eq 4. [g] This parameter was held fixed during nonlinear least-squares fitting of the $Br_{6,7}PC$ data.

1), suggesting the occurrence of pronounced fluctuations in the depths of the pyrenes and/or the bromine atoms. However, upon addition of 50 mol % cholesterol to the bilayers, the distributions undergo a significant narrowing, with h decreasing to a mean value of ≈5.7 mu. This is not an unexpected result, since cholesterol is known to force the acyl chains toward the all-trans conformation (Davies et al., 1990; Mendelsohn et al., 1991), thus increasing the transversal localization of pyrenes and bromines. A similar effect of cholesterol was observed in the previous conformation study (Eklund et al., 1992) as well as in work utilizing ^{14}N and ^{15}N stearic acid spin-label pairs and the electron−electron double resonance technique (Yin et al., 1987). We note that this method of analysis of the quenching data has the advantage of being insensitive to any variations in the degree of bromination of the quencher lipids, since the distribution parameters are optimized separately for each bromolipid. However, this procedure can only provide distribution parameters that are averages over all pyrenyl acyl chain lengths.

In order to characterize the distribution of the pyrenyl moieties for each individual Pyr_nPC, we used a second approach to the analysis of the data. This consisted of plotting the K_{SV} values for each Pyr_nPC *versus* b, the averages of the positions of the two bromine atoms in each of the three $Br_{x,y}PCs$ used, and fitting them to eq 4. The resulting parameters (not shown) were, however, inconsistent with those obtained from the first method. The reason for this inconsistence becomes clear upon inspection of Figure 4 and Table 1: the value of K_{max} is not constant for all $Br_{x,y}PCs$ but decreases markedly as the bromines are moved down the chain, suggesting a loss of effectiveness of the deeper quenchers. One possible explanation for this change in K_{max} is that the presence of the bromine atoms at the shallower positions may increase the packing disorder in the bilayer and enhance vertical fluctuations of the bromines and/or the pyrenes, with a consequent increase in the frequency of pyrene−bromine collisions. Such depth-dependent bilayer disordering by bromines has been previously suggested (McIntosh & Holloway, 1987). Another possibility is that the distributions of the deeper bromines may be wider than those of the shallower ones, resulting in lower quencher concentrations at the nominal depths defined by their attachment points. Although at odds with the conclusions reached by McIntosh and Holloway (1987) on the basis of their X-ray diffraction analysis, this argument is supported by other evidence, such as the decrease in the values of the segmental order parameters for methylene units deeper than the eighth (Seelig & Seelig, 1980) and the recent results of molecular dynamics simulations (De Loof et al., 1991; Pearce & Harvey, 1993). However, regardless of the mechanism responsible for the observed variation in K_{max}, normalization of the set of K_{SV} values for each $Br_{x,y}PC$ using the respective K_{max} listed in Table 1 is expected to yield parameters free from its effects. The normalized data, shown in Figure 5, were fit by means of the following two-parameter Gaussian equation:

$$K_{SV} = e^{-[(n+d-b)/h]^2} \quad (5)$$

The best fits to this equation, calculated with the optimized parameters listed in Table 2, are plotted as continuous lines in Figure 5. Despite the spread in the individual values, this

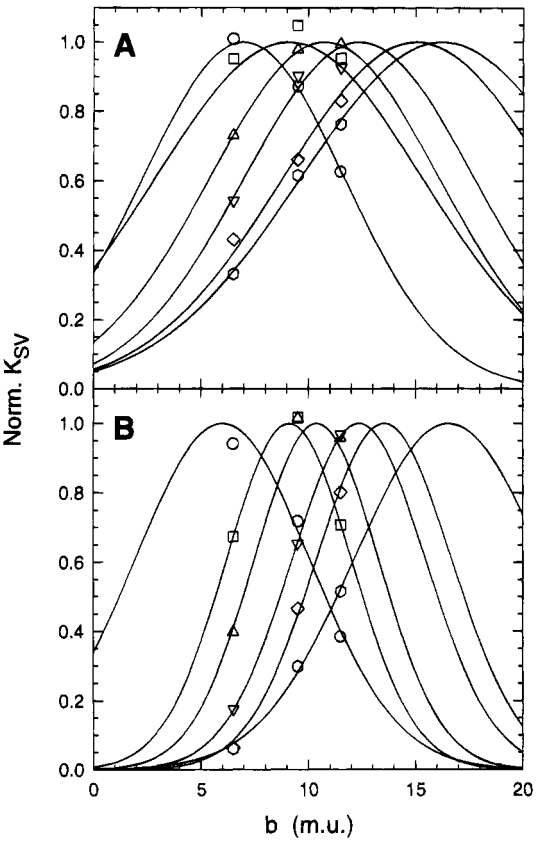

FIGURE 5: Dependence of the normalized K_{SV} values on b, the distance in mu, from the bilayer−water interface to the midpoint between the two bromine atoms in the *sn*-2 acyl chain of $Br_{x,y}PC$. The bilayers contained no (A) or 50 mol % cholesterol (B). The symbols for the various Pyr_nPCs are the same as in Figure 3. The normalized K_{SV} values were calculated by dividing the experimental K_{SV} values by the respective K_{max}, listed in Table 1, obtained for each $Br_{x,y}PC$ matrix from the fits shown in Figure 4. The lines are the best fits to eq 5 using the parameters listed in Table 2. The lines for Pyr_6PC and $Pyr_{12}PC$ in panel A were calculated using the d values obtained from the fits in which h was held fixed at 8.8 mu.

procedure yields results generally consistent with those obtained from the first method of analysis, as indicated by the similarity in the mean values of d and h listed in Tables 1 and 2. Also in agreement with the results of the first method, addition of 50 mol % cholesterol to the bilayers results in a marked narrowing of the apparent pyrene distributions without any significant shift in the average depths of the pyrenes (Figure 5 and Table 2).

The values of h obtained for the Pyr_6PC and $Pyr_{12}PC$ distributions in the absence of cholesterol, and for the Pyr_4-PC and $Pyr_{14}PC$ distributions in the presence of cholesterol, appear to be significantly wider than all the others. These results are probably due to one or more of several factors, such as experimental uncertainties, absence of clear peaks or small range of values in the data sets, or relatively low quenching rates: since each Gaussian is defined by only three data points, even a relatively small change in the value of a single data point may produce a considerable effect on the parameters.

From the preceding discussion, it is evident that the accuracy of the present Gaussian distribution analysis is limited by the small size of each individual data set, which depends on the number of available brominated lipids. Of course, the best solution for this shortcoming would be to

Table 2: Pyrene Distribution Parameters Obtained from the Dependence of the Normalized Values of K_{SV} on b, the Average of the Depths in mu of the Two Bromine Atoms in each $Br_{x,y}PC$

	POPC[a]				+50 mol % cholesterol[b]			
	d^c (mu)	h^d (mu)	$h_{pyr}{}^e$ (mu)	a^f (Å)	d (mu)	h (mu)	h_{pyr} (mu)	a (Å)
Pyr_4PC	3.0	6.7	4.7	6.3	2.0	5.8	4.1	6.5
Pyr_6PC	3.1 *(3.1 g)*	11.4	8.0	8.2	3.1	4.1	2.9	9.8
Pyr_8PC	2.7	7.6	5.4	9.7	2.4	4.1	2.9	11.2
$Pyr_{10}PC$	2.4	7.6	5.4	11.1	2.4	4.4	3.1	13.4
$Pyr_{12}PC$	4.1 *(3.0 g)*	10.4	7.3	14.5	1.5	4.5	3.2	14.6
$Pyr_{14}PC$	2.2	9.4	6.6	14.6	2.6	6.3	4.4	17.9
mean	2.9 ● 0.7	8.8 ± 1.8	6.3 ± 1.3		2.3 ± 0.5	4.9 ± 0.9	3.4 ± 0.7	

[a] The bilayers consisted of POPC and $Br_{x,y}PC$ in variable molar ratios. [b] The bilayers consisted of POPC and $Br_{x,y}PC$ in variable molar ratios and 50 mol % cholesterol (cholesterol/phospholipid mole ratio = 1.0). [c] The effective distance of the pyrene center to the site of attachment to the acyl chain (see Figure 1). [d] The $1/e$ half-width of the pyrene Gaussian in methylene units: as discussed in the text, this value includes contributions from the physical sizes of pyrene and bromines, as well as broadening effects due to their motions. [e] The $1/e$ half-width of the pyrene Gaussian reduced by a factor of $1/\sqrt{2}$ (see Discussion). [f] Distance of the effective center of the pyrene moiety from the bilayer/water interphase (see Figure 1). It is assumed that 1 mu is equivalent to 0.9 Å in the absence of cholesterol (McIntosh & Holloway, 1987) and to 1.08 Å in the presence of cholesterol, on the basis of the 20% increase in bilayer thickness measured by X-ray diffraction (Lecuyer & Dervichian, 1969). [g] Value of d obtained from nonlinear least-squares fitting of the data while holding the parameter h fixed at the calculated mean value of 8.8 mu.

synthesize and use additional $Br_{x,y}PC$s to better define each function. An alternative strategy, and the third of our analysis methods, is to combine all the available data and to fit them to a single, "global" Gaussian function whose parameters are now overdetermined and much less sensitive to the experimental noise than those described so far. This is realized by plotting the normalized K_{SV} value for each $Br_{x,y}PC/Pyr_nPC$ combination as a function of the new independent variable $(n - b)$, as shown in Figure 6. If, as implied by the similarity of the mean values of d and h obtained by the two analysis methods described above, the quenching rate is a well-behaved function of the difference between the pyrene depth, $n + d$, and the bromine depth, b, then this combined data set should be well fit by a Gaussian function with center equal to $-d$ and with $1/e$ half-width similar to the mean values of h listed in Tables 1 and 2. This is indeed the case, as demonstrated by the continuous lines in Figure 6 representing the best fits calculated with $d = 2.53$ (±0.25) and $h = 8.69$ (±0.39) mu, in the absence of cholesterol, and $d = 2.57$ (±0.20) and $h = 5.24$ (±0.25) mu in the presence of 50 mol % cholesterol. The results of this "global" distribution analysis of the quenching data confirm and strengthen the conclusions derived from the two analysis strategies described above, as they clearly indicate that (i) the average depths of the pyrenyl moieties are determined by the lengths of the respective acyl chains plus an additional constant contribution from the size of the pyrene itself, (ii) these depths are largely unaffected by the presence of cholesterol, apart from the effect of the increased bilayer thickness, and (iii) the major effect of cholesterol is to reduce the widths of the distributions, as indicated by the 40% reduction in the value of h.

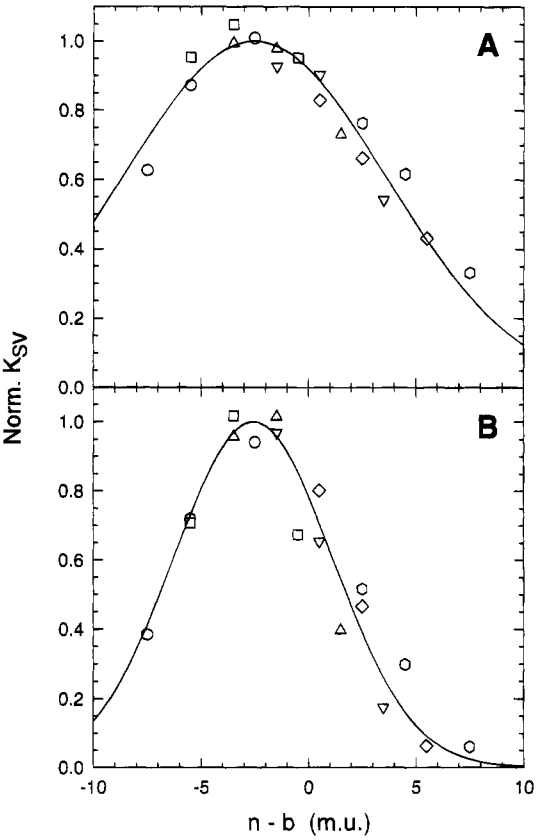

FIGURE 6: Dependence of the normalized K_{SV} values on $n - b$, the separation in mu between the point of attachment of each pyrene and the midpoint between the two bromine atoms in the *sn*-2 acyl chain of $Br_{x,y}PC$. The bilayers contained no (A) or 50 mol % cholesterol (B). The symbols for the various Pyr_nPC are the same as in Figure 3. The lines represent the best fits to a Gaussian equation with center equal to $-d$ and $1/e$ half-widths equal to h.

DISCUSSION

In this report, we have demonstrated that quenching of the fluorescence of a series of phosphatidylcholine analogues, bearing a pyrenylacyl chain of variable length in the *sn*-2 position, by dibrominated phosphatidylcholine quenchers is well modeled by assuming a Gaussian distribution for the depths of the pyrenyl moieties within the bilayer. A symmetric Gaussian function was used as an approximation of the actual distribution which, as suggested by the results of molecular dynamics simulations, may be skewed in shape (De Loof et al., 1991; Pearce & Harvey, 1993). Nevertheless, we believe that this method provides a more accurate description of the physical reality of the interior of the bilayer than the classical parallax method, which assumes pointlike distribution functions for both quenchers and fluorophores. The next level of refinement of the present distribution analysis method consists of devising a new procedure which takes into account explicitly the widths of the bromine distributions in the calculation of the probe distribution parameters. Such a procedure is currently under development in our laboratory, and its application to these data and

those published by other investigators will be the subject of a future report.

Our present analysis demonstrates that the average depths of the pyrenyl moieties are determined by the lengths of the acyl chains to which they are linked, as shown by the similarity of the parameter d for all Pyr$_n$PCs (Table 2). This confirms that the pyrene moieties have no intrinsic tendency to adopt a particular depth within the bilayer and to perturb the conformation of the acyl chains to which they are attached.

Another important result relates to the effect of cholesterol on the probe distributions. As shown in Tables 1 and 2 and by the results of the "global" analysis, the d values are not significantly affected by the presence of cholesterol, indicating that the average *separation* between probes and bromine atoms is not perturbed. In contrast, addition of 50 mol % cholesterol to the bilayers results in a marked narrowing of the depth distributions of the pyrenyl moieties. This result agrees well with the conclusions of our previous report (Eklund et al., 1992) and also with previous evidence that cholesterol forces the lipid acyl chains to adopt a more extended conformation by opposing the formation of *gauche* conformers (Seelig & Seelig, 1980; Davies et al., 1990; Mendelsohn et al., 1991).

It must be emphasized again that the pyrene Gaussian distributions defined in our analysis represent the result of the convolution of the individual bromine and pyrene distributions and, therefore, the reported values of h should be considered upper limits of the actual pyrene distribution widths. Since the convolution product of two Gaussians is another Gaussian with $1/e$ half-width equal to $(h_1^2 + h_2^2)^{1/2}$ (Wiener & White, 1991, and references cited therein), the lower limits of h can be found if we assume equal widths for both bromine and pyrene distributions: in this case, the values of h are reduced by a factor of $1/\sqrt{2}$, as listed in Tables 1 and 2 under the h_{pyr} heading. Finally, assuming a value of 5 Å $\cong$ 5.5 mu for the $1/e$ half-widths of the bromine atoms (Wiener & White, 1991) and using the convolution expression given above, the mean values of h in the absence of cholesterol, listed in Tables 1 and 2, are reduced to $\approx$7.0 mu. On the basis of these various estimates, it is likely that the true distribution widths of the pyrene moieties are considerably narrower than those given by h.

Abrams and London (1993) have provided evidence that acyl-linked anthroyloxy moieties may move toward the bilayer surface upon excitation, possibly as a result of an increased polarity of these fluorophores in the excited state as compared to the ground state. The lack of a similar behavior by the pyrenyl lipid analogues is likely due to the low polarity of the pyrene moiety even in the excited state.

Our results are also relevant to other applications which make use of pyrenyl lipid analogues. For instance, since the pyrene absorption spectrum overlaps extensively with the emission spectrum of tryptophan, Pyr$_n$PCs have been used as energy acceptors from tryptophan in RET studies of the transversal distribution of membrane-bound proteins (Vauhkonen & Somerharju, 1989; Bastiaens et al., 1990). Because of its inverse sixth power dependence on the donor–acceptor distance, the RET efficiency is expected to be very sensitive to the existence of depth distributions of the fluorophore moieties within the membrane. Ignoring such effects could result in large errors in the estimates of the average donor–acceptor separation distances. Thus, proper analysis of RET experiments making use of membrane-bound fluorophores should take into consideration the distributed nature of their positions, in analogy to the methods developed to account for the effects of intramolecular dynamics on RET measurements in water-soluble proteins and polymers (Haas & Steinberg, 1984; Amir & Haas, 1987). The characterization of the transversal distribution of the acyl-bound pyrenes should lead to more accurate estimates of the locations of protein tryptophans and other membrane-associated moieties capable of functioning as energy donors or acceptors with pyrene.

In conclusion, we have shown that the transversal distribution of a pyrene moiety attached to the terminal methylene unit of a phospholipid acyl chain is determined largely or, perhaps, exclusively by the length and conformation of the linked chain. The pyrene moiety, unlike more polar fluorophores, does not show an intrinsic tendency to partition to the bilayer surface and thus force the acyl chains into a distorted conformation. Therefore, pyrenyl derivatives are expected to mimic more closely their natural, unlabeled precursors. Finally, knowledge of the acyl chain length dependence of the distributions increases the uselfulness of the pyrenyl phospholipids for the localization of other fluorophores by the RET technique.

ACKNOWLEDGMENT

We thank Mr. Weidong Wang for carrying out the time-resolved fluorescent measurements, Dr. Heikki Väänänen for preparing Figure 1, and Drs. J. Eisinger and A. Ladokhin for helpful discussions.

REFERENCES

Abrams, F. S., & London, E. (1992) *Biochemistry 31*, 5312–5322.
Abrams, F. S., & London, E. (1993) *Biochemistry 32*, 10826–10831.
Abrams, F. S., Chattopadhyay, A., & London, E. (1992) *Biochemistry 31*, 5322–5327.
Amir, D., & Haas, E. (1987) *Biochemistry 26*, 2162–2175.
Bastiaens, P., de Beus, A., Lacker, M., Somerharju, P., Vauhkonen, M., & Eisinger, J. (1990) *Biophys. J. 58*, 665–675.
Bolen, E. J., & Holloway, P. W. (1990) *Biochemistry 29*, 9638–9643.
Chattopadhyay, A., & London, E. (1987) *Biochemistry 26*, 39–45.
Chong, P. L.-G., & Thompson, T. E. (1985) *Biophys. J. 47*, 613–621.
Davies, M. A., Schuster, H. F., Brauner, J. W., & Mendelsohn, R. (1990) *Biochemistry 29*, 4368–4373.
Dawidowicz, E. A., & Rothman, J. E. (1976) *Biochim. Biophys. Acta 455*, 621–630.
De Loof, H., Harvey, S. C., Segrest, J. P., & Pastor, R. W. (1991) *Biochemistry 30*, 2099–2113.
Dix, J. A., & Verkman, A. S. (1990) *Biochemistry 29*, 1949–1953.
East, J. M., & Lee, A. G. (1982) *Biochemistry 21*, 4144–4151.
Eisinger, J., Flores, J., & Bookchin, R. M. (1984) *J. Biol. Chem. 259*, 7169–7177.
Eisinger, J., Flores, J., & Petersen, W. P. (1986) *Biophys. J. 49*, 987–1001.
Eklund, K. K., Virtanen, J. A., Kinnunen, P. K. J., Kasurinen, J., & Somerharju, P. J. (1992) *Biochemistry 31*, 8560–8565.
Fischkoff, S., & Vanderkooi, J. M. (1975) *J. Gen. Physiol. 65*, 663–676.
Galla, H.-J., & Sackmann, E. (1975) *J. Am. Chem. Soc. 97*, 4114–4121.
Galla, H.-J., Hartmann, W., Theilen, U., & Sackmann, E. (1979) *J. Membr. Biol. 48*, 215–236.
Haas, E., & Steinberg, I. Z. (1984) *Biophys. J. 46*, 429–437.

Hendrikson, H. S., & Rauk, P. N. (1981) *Anal. Biochem. 116*, 553–558.
Hresko, R. C., Sugar, I. P., Barenholz, Y., & Thompson, T. E. (1986) *Biochemistry 25*, 3813–3823.
Kleinfeld, A. M. (1985) *Biochemistry 24*, 1874–1882.
Ladokhin, A. S. (1993) *Biophys. J. 64*, A290.
Lakowicz, J. R. (1983) *Principles of Fluorescence Spectroscopy*, Plenum Press, New York.
Lecuyer, H., & Dervichian, H. (1969) *J. Mol. Biol. 45*, 39–57.
Mason, J. T., Broccoli, A. V., & Huang, C.-H. (1981) *Anal. Biochem. 113*, 96–101.
McIntosh, T. J., & Holloway, P. W. (1987) *Biochemistry 26*, 1783–1788.
Mendelsohn, R., Davies, M. A., Schuster, H. F., & Bittman, R. (1991) *Biochemistry 30*, 8558–8563.
Pearce, L. L., & Harvey, S. C. (1993) *Biophys. J. 65*, 1084–1092.
Pownall, H. J., & Smith, L. C. (1989) *Chem. Phys. Lipids 50*, 191–211.
Robertson, J. M., & White, J. G. (1947) *J. Chem. Soc. (London)*, 358–368.
Roseman, M. A., & Thompson, T. E. (1980) *Biochemistry 19*, 439–444.
Rouser, G., Fleischer, S., & Yamamoto, A. (1970) *Lipids 5*, 494–496.
Sassaroli, M., Vauhkonen, M., Perry, D., & Eisinger, J. (1990) *Biophys. J. 57*, 281–290.
Seelig, J., & Seelig, A. (1980) *Q. Rev. Biophys. 13*, 19–61.
Somerharju, P., Virtanen, J., Eklund, K., Vainio, P., & Kinnunen, P. (1985) *Biochemistry 24*, 2773–2781.
Somerharju, P., van Loon, D., & Wirtz, K. W. A. (1987) *Biochemistry 26*, 7193–7199.
Tang, D., & Chong, L.-G. (1992) *Biophys. J. 63*, 903–910.
Tennyson, J., & Holloway, P. W. (1986) *J. Biol. Chem. 261*, 14196–14200.
Thuren, T., Vainio, P., Virtanen, J., Somerharju, P., Blomqvist, K., & Kinnunen, P. (1984) *Biochemistry 23*, 5129–5134.
Tretyachenko-Ladokhina, V. G., Ladokhin, A. S., Wang, L., Steggles, A. W., & Holloway, P. W. (1993) *Biochim. Biophys. Acta 1153*, 163–169.
Vauhkonen, M., & Somerharju, P. (1989) *Biochim. Biophys. Acta 984*, 81–87.
Vauhkonen, M., Sassaroli, M., Somerharju, P., & Eisinger, J. (1990) *Biophys. J. 57*, 291–300.
Virtanen, J., Sassaroli, M., Ruonala, M., Vauhkonen, M., & Somerharju, P. (1994) *Biophys. J. 66*, A288.
Wiener, M. C., & White, S. H. (1991) *Biochemistry 30*, 6997–7008.
Wiener, M. C., & White, S. H. (1992) *Biophys. J. 61*, 434–447.
Wolf, D. E., Winiski, A. P., Ting, A. E., Bocian, K. M., & Pagano, R. E. (1992) *Biochemistry 31*, 2865–2873.
Yin, J.-J., Feix, J. B., & Hyde, J. S. (1987) *Biophys. J. 52*, 1031–1038.

BI9502497